Comminution Simulation Using Discrete Element Method (DEM) Approach From Single Particle Breakage to Full-Scale SAG Mill Operation

Lawrence K. Nordell and Alexander V. Potapov*
Conveyor Dynamics, Inc.
*E-mail: nordell@conveyor-dynamics.com
and
John A. Herbst
Svedala Optimization Services

September, 2001

ABSTRACT

The Discrete Element Method (DEM) approach is used to simulate flow of granular materials for a variety of mining industry applications. The next step in this approach is to combine several DEM particles into particle clusters using structural bonds and to allow them to break to simulate the comminution processes. Current progress in computer technology and development of computer parallel algorithms allows us to perform large-scale 3-D DEM simulations of the comminution process. Examples of these simulations, applied to SAG mills, will be presented in graphical and animation form. Specific studies determining critical size and critical shape are presented.

INTRODUCTION

Three Dimensional (3D) Discrete Element Method (DEM) modeling will provoke major performance improvements, in mineral comminution, as this conference will attest.

Crushing and milling total performance advancements are highlighted in this and related SAG 2001 papers demonstrating the degrees of improvement, which are imminent (Herbst and Nordell, 2001, Qiu et al, 2001; Song et al, 2001).

We have advanced beyond the stages of "guesstimate" engineering, 2-D rhetoric, single-phase physics, mystic data analysis, and pseudo-empirical rules modeling.

Conveyor Dynamics, Inc., (CDI) was introduced to the art of milling by Palabora Mining Company in 1994. CDI developed the first conveyor belt hard rock curved chute to replace a conventional rock box design. The curved chute extended the belt's life from three years to a projected 20 years (Nordell, Van Heerden, 1997). Six years have passed which validate the prediction. Palabora suggested that DEM (granular mechanics) technology be applied to their 10m diameter autogenous (AG) mills. A mill drive pinion and lifter assembly were strain gauged, in 1995, to verify 3-D DEM predictions. Simulations demonstrated good agreement with power and lifter force toe through shoulder measurements. A lengthy studied period followed the initial work to incorporate: non-Newtonian fluid with a free surface, non-round polyhedral ore shapes, discrete grain breakage (DGB) of ore particles, from the work of Potapov (Potapov and C.S.Campbell, 1996), parallel computing, advance visualization techniques, and verification tools and codes (MILLSTAT: statistical analysis of instrumentation data archives, and MILLSIM: Mill Population Balance Model (PBM) circuit simulator), wear prediction, and laser measurements of wear surfaces. A close technical association with Svedala Optimization Services has brought us to the end-of-the-beginning with these research developments. Svedala is analyzing, validating, and applying these technologies and equipment developments.

This paper illustrates our DEM applications in comminution, ranges of comminution behavior, and the due-diligence program we have developed to: 1) identify and verify performance claims, and 2) optimize the comminution phase of the mineral production process.

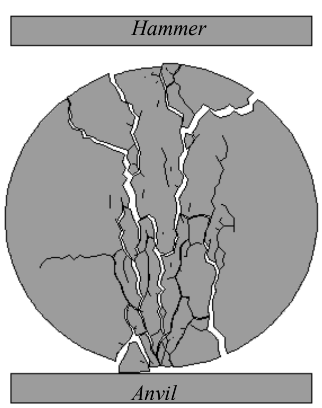

Figure 1. Impact fracture of single particle – magnitude 1X.

Figure 2. Impact fracture of single particle – magnitude 4X.

Comminution basics start with a single particle. Figure 1 illustrates the DEM breakage model (discrete grain breakage, denoted at DGB), developed by Potapov (Potapov and Campbell, 1996). A laboratory rock is hit by a hammer. The hammer's energy breaks the rock, exposing surface area. From the initial mass, rock properties, impact energy, liberated surface measurement, and test procedures, a surface energy parameter is defined. The surface energy contains information on rock strength, hardness, fracture toughness, grain boundaries, and prior rock structural damage.

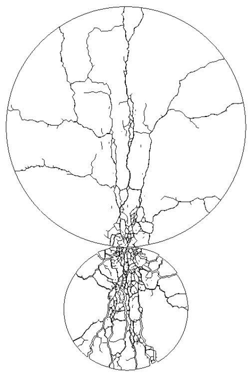

Figure 3. Impact fracture with different particle sizes

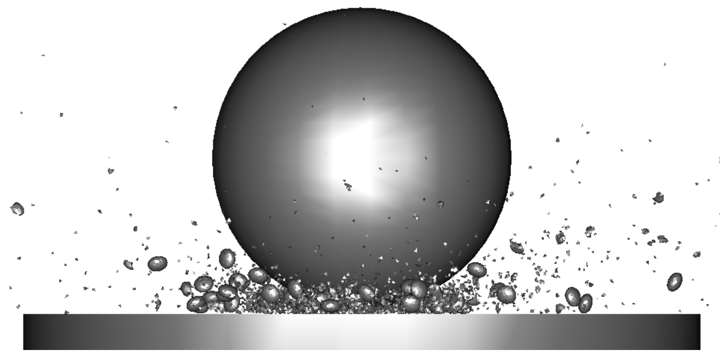

Figure 4a. Impact fracture of particle bed

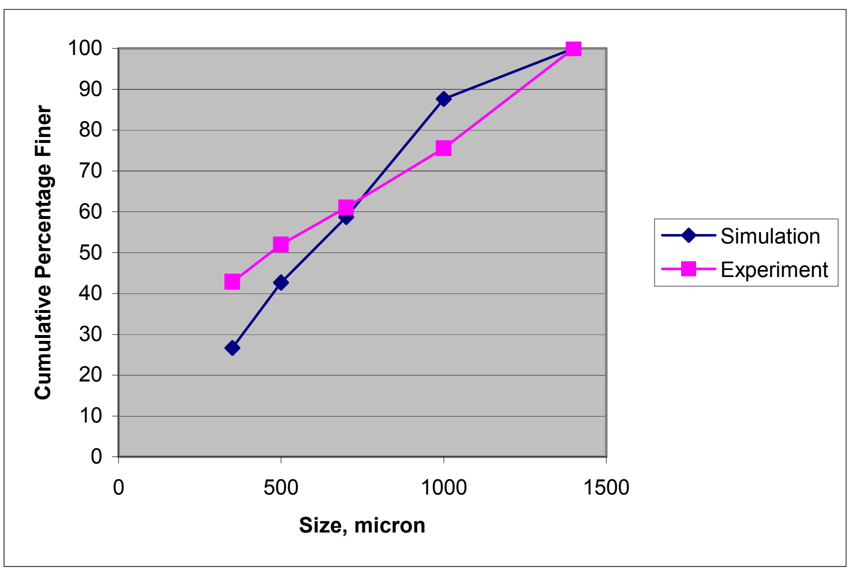

Figure 4b. Figure 4a compared with lab experiment.

Figure 2 illustrates the DGB model when the impact energy is increased four fold. Figure 3 shows fracture behavior on collision with unequal sizes. Figure 4a is a study of rock fracture in a particle bed. Figure 4b is the graphical comparison between a measured fractured particle bed and DGB results from Figure 4a. The DGB particles were of uniform oblate shape. The experimental bed had a larger distributed size range with irregular shapes that were consolidated before impact.

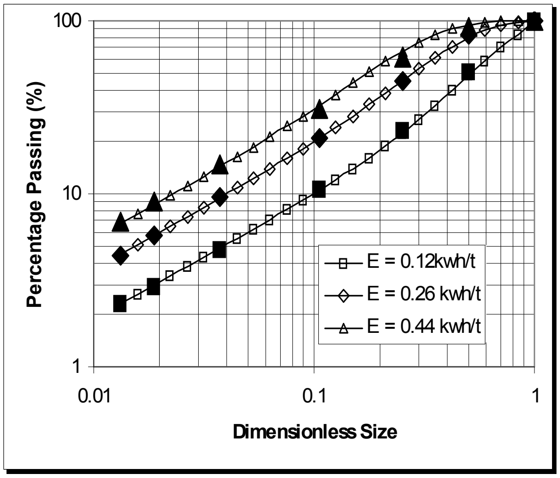

Figure 5. three impact ore size reduction vs. impact energies comparing lab measurements with theoretical equation

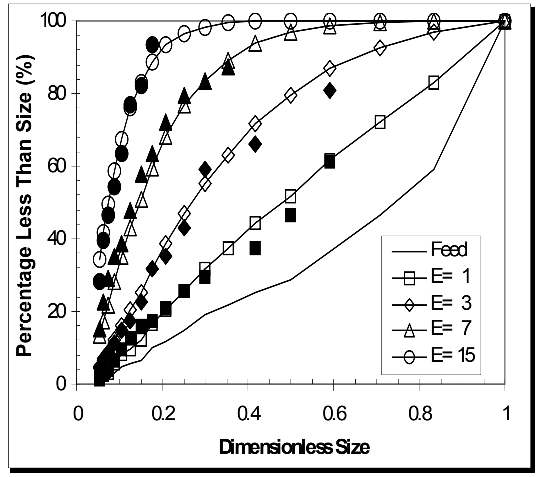

Figure 6. Ore size (hollow points: CDI Energy Model, solid points: CDI Particle Fracture Model)

We study single particle breakage to tune rock fractures for both the DGB model and for the breakage (appearance) function in the PBM (MILLSIM) model. Figure 5 illustrates experimental ore breakage versus DGB for three impact energy levels in kilowatt hours/ton (Kwhr/t). The x-axis represents the ratio of the progeny size, from breakage, relative to the parent's original size (1.0). The y-axis represents the accumulative percentage screen passing size.

The dots are the laboratory measurements. The lines through the dots represent one rock energy breakage equation that unifies the breakage behavior of this rock group, over a 100:1 size range, for varying impact energy levels. This equation defines the breakage function (B) in our PBM code (MILLSIM).

Figure 6 shows a comparison of the PBM breakage function (B) with the DGB code over the range of 15 to 1 impact energy levels. Percent passing, versus relative reduction in rock size is plotted. This graph demonstrates that the DGB and PBM breakage function appears to be unified. The results compare with the results of R. P. King (King et al, 1997).

UNIFYING PBM AND DEM

In order to complete the unification of PBM with DEM, we must be able to represent multiple ore strengths and define the attributes of the selection function (S). This is far more complex than the breakage function (B).

Attributes within and about the mill assembly that must be identified and quantified are:

1) ore size distribution
2) frequency and energy spectra of collisions between ore particles of all size groups, ore and ball collisions, and ore and lifter/liner collisions
3) collisions that induce breakage – impact and shear

4) rock shapes by size and type (strength; density)
5) orientation of rocks during collisions
6) ball charge (volume: ball sizes, shapes; density; aspect ratio)
7) slurry rheology with axial and radial flow influence on ore charge dynamics
8) pan lifter/liner geometry
9) entry and exit pan lifter geometry
10) exit grate geometry and open grate area by location
11) ore recycling into mill and within pan cavity
12) ore flow efficiency on mill trommel
13) slurry recycling from the pan cavity
14) slurry axial velocity in mill and through grate
15) mill speed
16) ball to ore ratio
17) ore recycle – trommel oversize, recrush; fines in recycle

The DEM model, with and without breakage, can define and/or represent the noted 17 attributes, with varying accuracy associated with cost and timing. Based on the DEM refinements, the PBM model selection function (S) can be refined to more accurately represent the ore breakage transformation and stochastic impediments.

As noted from the publication by Wayne Stange (Stange, 1996), when binary or multi-strength ores are present, misrepresentation of dual breakage functions leads to gross errors in estimating the charge size distribution. DEM analysis of ore charge dynamics and resulting energy breakage spectra, by size, must have an accurate size distribution by ore strengths, shapes, and densities. Therefore, the PBM and DEM are strongly dependent on each other to resolve collectively the weakness in each. PBM needs ore, ball, and slurry characterizations, convection, impact and shear energy spectra, and recycling behavior. DEM needs the size distribution.

DEM influence on the PBM model's accuracy can be shown in the following illustrations of: 1) lifter and particle shape and, 2) exit grate/ pan cavity flow and recycling dynamics.

MILL LIFTER AND PARTICLE SHAPE INFLUENCE ON COMMINUTION

What is/are the dominant AG/SAG mill comminution process(es) for most hard rock with Bond work index >8? Four examples are presented, in Figure 7, to qualitatively illustrate how mill liner and ore shape influences the comminution process. These examples illustrate comminution behavior in a mill with angular polygonal shaped ore.

1) new 66 lifter set with 9 degree face angle
2) new 33 lifter set with 9 degree face angle

3) worn 66 lifter set worn with about 45 degree face angle
4) new 66 lifter set, same as example 1, except beginning with rounded particles

The mill configuration, in Figure 7, represents a typical 10.4m diameter (34-foot) SAG mill. The image is taken after a representative amount of ore is broken to illustrate key behaviors. Ore breakage rates, dependent on lifter and ore geometry, are noted. Comparative energy used to achieve these relative breakage rates is also noted.

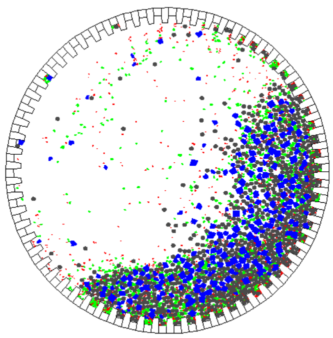

Figure 7a. New with 66 lifters

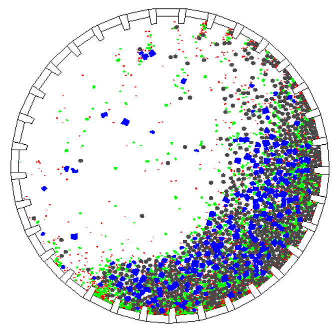

Figure 7b. New with 33 lifters

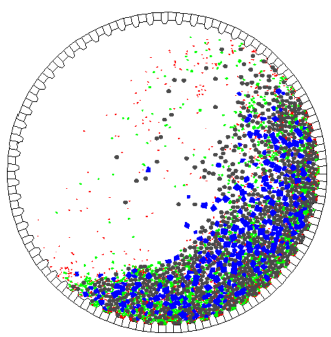

Figure 7c. 75% worn with 66 lifters

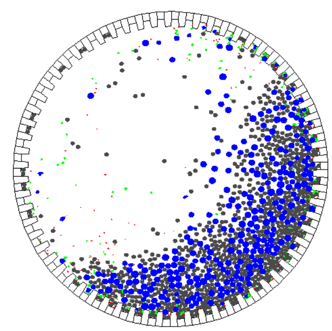

Figure 7d. New with 66 lifters – round ore

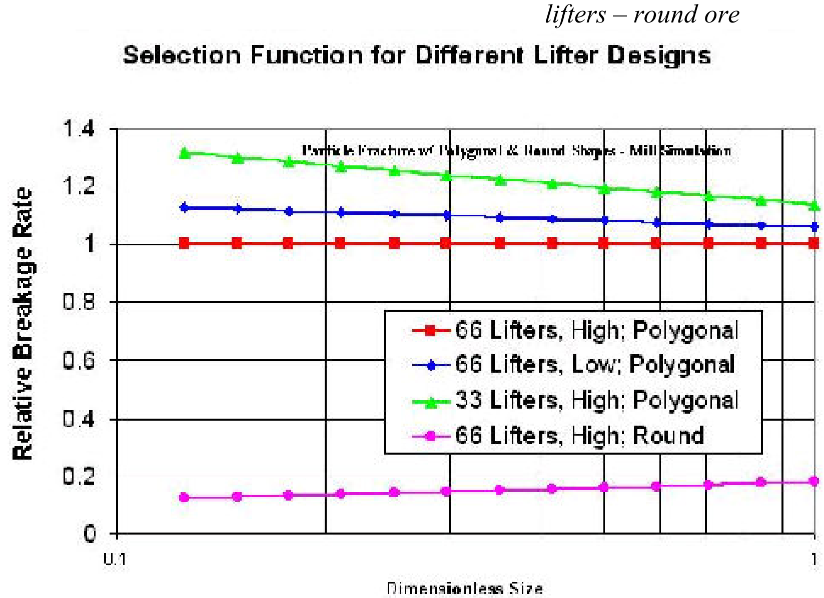

Figure 7e. Breakage rates for 7a through 7d.

Discrete grain breakage simulates ore comminution for 2.0 mill revolutions. Charge volume is 12-percent ore at about 210 mm passing size, and 12-percent ball at 133mm (5.25inch) ball size. The mill was run to steady state with uniform ore and ball mixing before breakage was activated. Reasonable size distribution was achieved after 2.0 revolutions.

Figure 7a is the basis for comparison. The 10.4m mill has 66 lifters at about 240mm high by 9-degree face angle. Highlights are: 1) ball and particle impact trajectory has many ball and ore impacting near 9 o'clock on the mill wall; 2) ball and ore packing are prevalent.

Figure 7b illustrates the change in charge behavior, from Figure 7a, when the lifters are still new but with every other lifter removed. Ore and ball packing are replaced by ball and ore stacking. However, the general trajectory is similar to Figure 7a. Power consumption is increased about 4%. The breakage rate is increased about 20%.

Figure 7c illustrates Figure 7a with worn lifter behavior. The ore charge slumps. The ball impact trajectory, on average, falls about 45 degrees with a 45 degree face angle. Occasionally, balls hit around 8 o'clock, but most impact is nearer to 7 o'clock. The power increases about 10% and the breakage rate increases about 8 percent.

Figure 7d illustrates mill behavior from Figure 7a, when rocks become rounded. Power consumption drops about 7%. The breakage rate is dramatically dropped to 13% of the base case in Figure 7a. This important point demonstrates, for this ore size and strength, sufficient impact breakage (joules/kg) is non-existent. The dominant comminution mechanism is chipping. Impact breakage will not become noticeable until the ore size is significantly below grate passing size. Even then it is not the major size reduction mechanism.

When ore becomes rounded in most AG/SAG mills, comminution is reduced in proportion to the relative size and quantity of rounded edges. Recycle crushers place edges on rock to induce comminution in AG and SAG mills. Mill design and PBM models must account for this condition.

Figure 7e is a graph of the breakage rates for Figures 7a through 7d respectively. All breakage rates for each size reduction in Figure 7a, have been normalized to unity. All other conditions are normalized by the multiple of Figure 7a breakage rate by ore size.

Figures 7a and 7d are indicative of the changes in comminution behavior due to mill and ore shapes. This is a qualitative representation.

Operators often identify increases in production with the wearing of mill lifter/liner and end grate openings. DEM modeling of rounded and worn lifters can identify the same conditions.

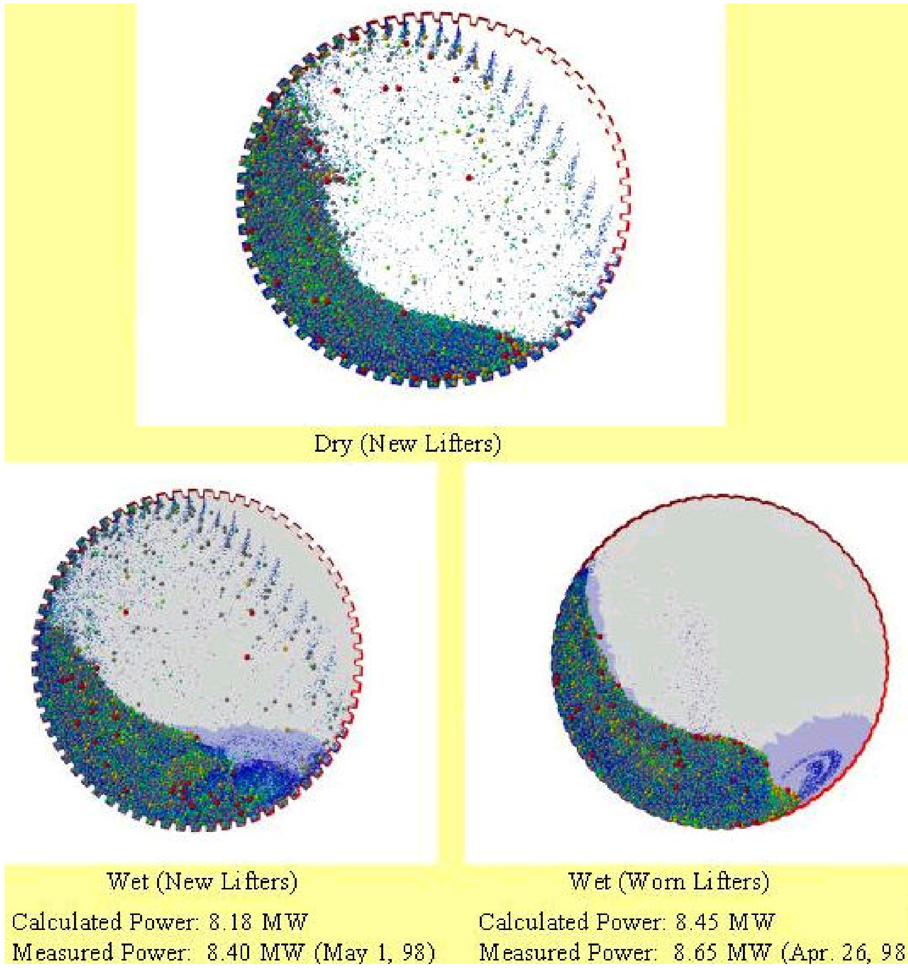

Figure 8

Figure 8 shows the behavior in a 66-lifter SAG mill, between 3-D DEM (non-breakage) models of a dry and wet (slurry) mill with new lifter shapes, and between a wet mill with new lifters and with worn lifters. Points of interest are: 1) comparing wet and dry mills with new lifters shows the slurry addition causes the charge to slump, 2) overall trajectory is nearly the same wet or dry, 3) DEM agrees with field measurements, 4) worn wet mill consumes 3% more power than when the lifters are new, 5) heavy cataracting does not exist with the worn mill, 6) the wet mill charge shoulder rides higher up the mill wall in the direction of rotation, and 7) although not shown, the worn mill comminution was over 5% higher.

Figures 9 and 10 illustrate comminution behavior over lifter-liner wear life. MILLSTAT (Song et al, 2001) produced the illustrated throughput data for lifter–liner life on two large SAG mills. Each mill was equipped with new lifters.

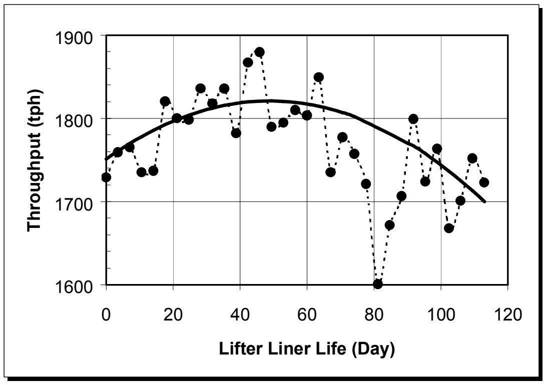

Figure 9. lifter performance is new life in Mill No. 1 MillStat Data Analysis

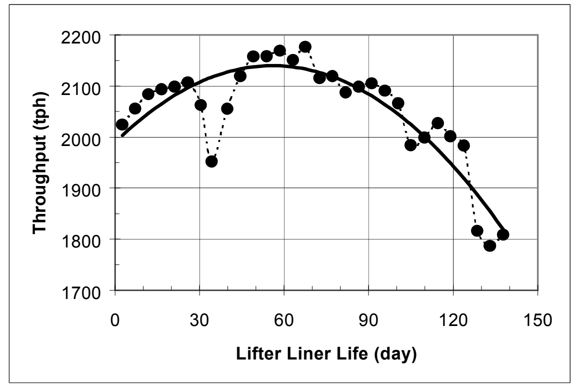

Figure 10. Lifter performance is new life in Mill No. 2 MillStat Data Analysis

The two mills' shapes, sizes, and ores differ. Performance peaks to 4% and 7% respectively at 44% of lifter wear life. Throughput is at par at 78% and 86% lifter wear life. At 100% of wear life, throughput drops 3% and 9% respectively, at which time the lifters are replaced. Similar results have been noted with CDI DEM analysis of client mills.

There exists an optimal lifter configuration that maximizes comminution, over the lifter life, dependent on:

1) face angle or curvature
2) lifter height
3) crown radius
4) root radius
5) lifter pitch
6) crown width
7) symmetric vs. non-symmetric liter shape
8) high:high / high:low patterns
9) ball size, shape, and density
10) ore size and strength distribution
11) ball to ore ratio
12) charge volume
13) mill bolt and shell strength limitations
14) slurry rheology and volume
15) mill rpm
16) lifter (metal) volume in mill

PERFORMANCE VERIFICATION

Many verification tools validate DEM and DGB in terms of: power, throughput, wear rate and shape, wear measurement, archive and online analysis of instrument database, and reasonably accurate PBM mill circuit simulation models (Svedala's MinOOcad and CDI's MILLSIM).

Table 1 presents a comparison of the well-known Chester Rowland formulation for ball mill power analysis versus our 3-D DEM model. A large ball mill power analysis study was completed. The study was over the range of 72-78% critical speeds (PCS) and 35-41% ball filling. The two methods differ by less than 2%.

Table 1: Power Prediction by DEM
Mill Power in MW (C. Rowland prediction in parentheses)

	% Ball Filling		
PCS	35	38	41
72	14.8 (15.2)	15.5 (15.8)	16.3 (16.2)
75	15.4 (15.7)	16.2 (16.3)	16.9 (16.9)
78	15.8 (16.2)	16.7 (16.8)	17.6 (17.4)

Accurate analysis of the mill shape is critical to developing DEM, PBM (MILLSIM) and MILLSTAT, tools that verify the cause and effect performance.

CDI has built laser shape measurement scanners for gyratory crushers and AG/SAG and ball mills. The scanners are accurate to within 1 mm on absolute distance, for both crusher mantle and concave wear profiles, and for mill lifter-liners over the length of the mill. The laser records data at about 2mm intervals across the scanned surface.

Figure 11 is a photo of the mill scanner assembly. The laser head shoots the mill cross-section at about 30,000 points per revolution in about six seconds. The mill can be scanned at 200mm axial intervals in about 15 minutes, once the equipment is in place.

Figure 12 is a plot of the laser scan, in a 10m mill, at three positions. Even with the printed image of this paper, one can detect irregularities that otherwise might go undetected.

Figure 11. – Mill Laser Scanner fully assembled – 4 meter bar length

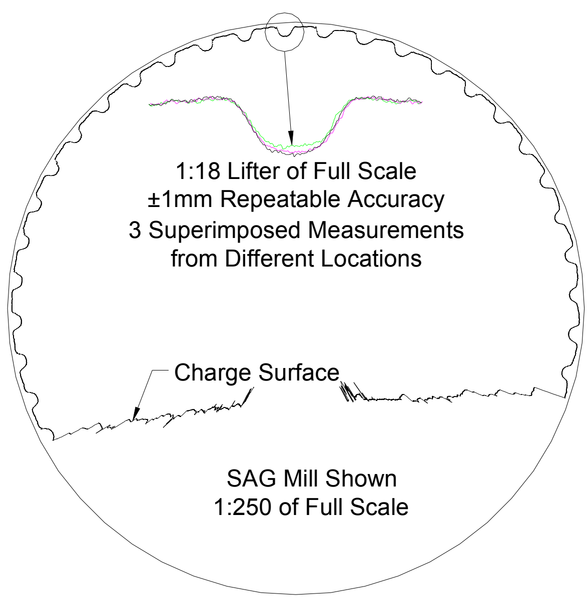

Figure 12. – Laser Scanner Measurement – SAG Mill Cross Section

A CDI laser scanner and tracking bar was positioned within a 60 x 89 gyratory crusher. Figure 13 shows the graph of new and worn mantle and concave images. X-Y plots resolve the crusher mantle and concave surfaces within 1mm of accuracy. The upper graph is the mantle as new and with a large worn zone near the close setting aperture. A line is placed across the worn zone that gives measure to the degree of wear. The lower plot is the concave, which can be distinguished from the mantle by the calibration rod spikes. The middle line between mantle and concave is the position representing the scanner guide or tracking bar. Comminution changes with wear can be explained and modified. New shape strategies with DGB can be theoretically analyzed without operational risks, and the results can create new strategies and geometries, which will improve the comminution.

Figure 13. Laser scanner measurements.

MILLSTAT, as reported in this conference (Song et al, 2001), is a powerful tool for analyzing mill statistical data. MILLSTAT filters data noise and statistical out-liers, organizes the attributes chronologically and/or between one or more independent variables to discern significant details in performance, and perform various regression formulations to ascertain trends of significance, and to couple data to simulation codes (MinOOcad and MILLSIM). The results of DEM and MILLSIM simulations would otherwise be subject to criticism.

DGB can analyze and sub-model special regions of comminution that can then be applied as rules for the more conventional 3-D DEM.

MILLSIM can verify DEM performance by comparing many attributes of the selection function(s) previously mentioned.

Probably the most important verification tool is the wear model results (Qiu, et al, 2001). CDI wear theory and field measurements are shown to be in close agreement over the lifter-liner life for a variety of mills, lifter shapes, ore types, and materials of construction. Wear history captures all aspects of granular mechanics and its dynamics as the wear profile changes, comminution changes and operator control set points change.

ORE BOTTLENECKS TO OPTIMAL THROUGHPUT

Regardless of comminution advancements with new lifter designs, enhancements in ball size and quantity, understanding and controlling slurry rheology, mill operations and its circuit balance, there are other mill components that will restrict performance. The main inhibitors are: 1) exit grate and its placement, 2) exit grate pan lifter shape and placement, 3) exit grate pan cavity and cone design, and 4) trommel design.

Exit grate opening design and placement, with respect to the pan lifter design and associated charge dynamics, can enhance or inhibit flow through the grate. Design improvements are being studied that consider a different style of grate.

Exit grate pan lifter shape inhibits mixing of ore sizes, which can pass through the grate. The large lifter shape (wear bars) stalls granular circulation once the charge fills the void near the grate. Eventually, the pan lifter radial edges are worn round, which increases flow circulation at the grate face, and the probability of fines accessing the openings. This problem is similar to the mill's axial lifter action. They do a better job with their edges rounded, enhancing circulation (increasing the selection function index).

Exit grate pan cavity, exit cone, and grate opening design may cause undesirable recycling of ore back into the mill. Figure 14 illustrates ore flow recycling in the pan cavity and back through the grate openings. Centrifugal force holds a significant amount of charge at the mill perimeter until the mill pan cavity positions the ore charge where the gravity force overcomes the centrifugal force. Flow begins to move toward the mill center and exit cone when the polar position reaches about 1 o'clock during clockwise rotation.

As the ore flows toward the mill center, it is restricted by two conditions. First, flow of multiple pan cavities converging at the beginning of the exit cone, where space limits the free flow of ore. Second, by the loss of the gravity force as the main ore flow reaches the exit cone when the mill is positioned at 3 o'clock. After 3 o'clock, no gravity force aids flow and the remaining ore is pulled back into the pan cavity. This recycling action is magnified as speed is increased. A study for a SAG mill client showed at 78% of critical speed, the DEM model predicts pan cavity recycling is about 75% of production. At 82% of critical speed, it may increase to over 200%.

The right image of Figure 14 shows recycling of product back through the grate as mineral passes over the grate as the pan cavity swings over 12 o'clock. The same DEM study indicates that at 78% of critical speed, about 27% of the ore flows back through the grates. At 82% of critical speed this may increase to 40%.

Figure 14: Ore recycling in pan cavity at left and flowing through grates back into mill at right.

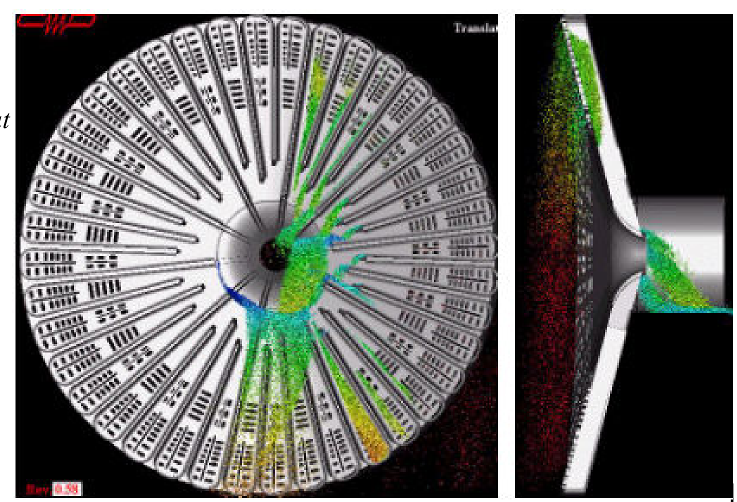

FULL SCALE MILL SIMULATION

The full-scale 3-D DEM mill image cutaway is presented in Figure 15. Many attributes of the full mill charge behavior, not previously reported, are being unveiled. Explanations of wear patterns, regions of high and low comminution, high power demand of the end cones are reported in Herbst (Herbst and Nordell, 2001). Many exciting findings may lead to major performance improvements, including increased comminution, reduced power consumption, and increased wear life. Enhanced flow of product through the grate will be among the major contributions.

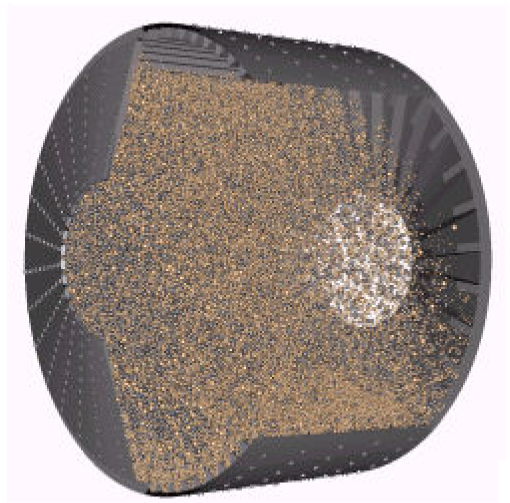

Figure 15. Full-scale 3-D DEM model of SAG Mill.

This paper presents the results of ongoing research at Conveyor Dynamics, Inc. (CDI), with the support of Svedala Optimization Service's intellectual and commercial resources. Highlights of our development are: two and three dimensional Discrete Element Modeling, DEM with granular breakage, termed Discrete Grain Breakage (DGB), Population Balance Modeling and flowsheet simulators (PBM using MillSim and Svedala's MinOOcad), statistical analysis of field instrument records (MILLSTAT), and mill laser scanning measurement equipment, and the association with our wear modeling techniques.

We predict the commercial benefits of this science will soon astound the mining industry.

ACKNOWLEDGEMENTS

Drs. John Qiu and Ming Song of CDI have participated fully in this research, and have made fundamental contributions. Their integral involvement in this ongoing work is key to its ultimate success. The critical support of Svedala is gratefully acknowledged and much appreciated. Without their dedication this rate of advancement would not be possible.

REFERENCES

Herbst, J. A. and Nordell, L.K., 2001, "Optimization of the Design of SAG Mill Internals Using High Fidelity Simulation", **Autogenous and Semiautogenous Grinding Technology: SAG 2001**, Editor, A. Mular.

King, R. P., et al, 1997, "Establishing the Energy Efficiency of a Ball Mill", **Comminution Practices**, Editor, S. K. Kawatra, SME.

Nordell, L.K. and Van Heerden, J.J., October 1995, "Curved Chutes and Other Improvements at the Palabora Mine", BELTCON 8, South Africa.

Potapov, A., Campbell, C., 1996, "A Three-dimensional Simulation of Brittle Solid Fracture", **International Journal of Modern Physics C**, Vol. 7, No. 5, pp.717-729.

Qiu, X., et al, 2001, "Prediction of Wear of Mill Lifters Using Discrete Element Method", **Autogenous and Semiautogenous Grinding Technology: SAG 2001**, Editor, A. Mular.

Song, M., et al, 2001, "MILLSTAT – A Software Package for Statistical Analysis of Mill Data Bases", **Autogenous and Semiautogenous Grinding Technology: SAG 2001**, Editor, A. Mular.

Stange, 1996. "The Modeling of Binary Ore Behavior in FAG/SAG Milling," **Autogenous and Semiautogenous Grinding Technology: SAG 1996**, Editors, A. Mular, D. Barratt, and D. Knight.